POLITECNICO DI TORINO
Repository ISTITUZIONALE

Robust control of a reverse-flow reactor

(Article begins on next page)

23 June 2024

Robust control of a Reverse-Flow Reactor

Davide Fissore[*], Antonello A. Barresi

Dipartimento di Scienza dei Materiali e Ingegneria Chimica, Politecnico di Torino,

C.so Duca degli Abruzzi 24, Torino, 10129, Italy

[*] Corresponding author: e-mail: davide.fissore@polito.it, Tel: +39-011-5644695, Fax: +39-011-5644699

Abstract

This paper is focused on the design of a robust controller for a catalytic fixed bed reactor with periodical inversion of the flow direction (Reverse-Flow Reactor, RFR). The analogy between the RFR operated at infinite switching frequency and the countercurrent reactor is the basis of the simplified mathematical model of the reactor.

The control system uses dilution and internal electric heating to ensure complete conversion of the reactants and to prevent overheating of the catalyst. As the state of the system is not fully available, apart from some temperature measurements, an observer is designed and used in the control algorithm. This is a typical case of non-linear system with uncertainties. Following the procedure described in detail by Fissore (2007), the extended model for the process is set-up, thus taking into account all the simplifications of the model and linking performance and robustness to the control law, which is a simple state feedback. Simulations with randomly varying feeding concentration have been carried out in order to demonstrate the effectiveness of the proposed control system.

Keywords

- Control of RFR
- H_∞ control
- Robust control
- Robust performance
- Observer design

Introduction

In the last decades a great interest grew up in the Chemical Engineers community towards the unsteady-state reactors; various configurations and a lot of processes that can take some advantages from this mode of reactor operation were investigated. Among the others, the attention of the researchers was focused on the catalytic Reverse-Flow Reactor (RFR), i.e. a fixed-bed catalytic reactor where the feeding direction is periodically reversed by acting on a set of valves. The RFR allows, for example, the autothermal combustion of cold and lean mixtures of air and VOC (Volatile Organic Compounds): no auxiliary fuel is needed except in the start-up phase when the catalytic bed is pre-heated (see, for example, the reviews of Matros and Bunimovich, 1996, and of Kolios et al., 2000). With a proper choice of the switching time (i.e. the time occurring between two successive inversions of the feed direction) a dynamic regime is obtained, with a "hot" zone located in the central part of the bed, where the reaction occurs, and a "cold" zone at the boundaries of the bed, where no reaction take place (and thus the catalyst can be replaced by an inert solid).

Beside the intrinsically dynamic behaviour of the RFR, one must deal with external perturbations (in the feed concentration, composition, temperature and flow rate) which may lead either to reactor extinction (and thus to the emission of unconverted reactants) or to catalyst overheating (and thus deactivation). Despite the large number of papers dealing with the various issues concerning the design of a RFR (mathematical modelling, parametric sensitivity analysis, process optimisation, experimental investigation and scale-up, ...), little attention was paid to the design of efficient monitoring and control systems (Barresi and Vanni, 2002a, 2002b; Edouard et al., 2005a, 2005b; Hevia et al., 2005; Fissore et al. 2006). The design of an efficient control system is of outmost importance for the reverse-flow catalytic afterburners where the feeding concentration changes with time. Feed flow-rate can also be variable, but in the industrial application the reactor is generally designed to operate at a constant flow rate (given by a blower) and thus only the response to changes in

2

the feeding concentration will be investigated in this paper.

Figure 1 shows a sketch of the catalytic RFR which is investigated in this work. The packing is made of two sets of monoliths: a long inert monolith and a short catalytic one. The geometrical characteristics (as well as the physical properties of the support and of the feeding) are the same of the system investigated by Ramdani et al (2001) and can be considered representative of an industrial apparatus. The wide square cross section of the monoliths prevents heat losses over their whole length; conversely, heat loss through the reactor wall takes place in the central chamber where the electrical heater is located and where fresh air can be injected for control purposes.

Our study is motivated by the results of Edouard et al. (2005a, 2005b) who investigated the possibility of using state-space based controllers, and in particular the Linear Quadratic Regulator, for the reactor of Figure 1: they pointed out that a lot of simplifications are required to apply this technique, thus questioning about the need for an accurate and complex model-based control algorithm in presence of a very simplified model. Even if they say that the errors due to the linearization can be considered negligible, all the algorithm is based on the assumption that the reactor is operated at high switching frequency, thus exploiting the analogy between the RFR and the countercurrent reactor (Nieken et al., 1995), and this may be questionable.

Robust control can be an interesting technique for designing a state-space based controller, taking into account model uncertainties. Christofides and Daoutidis (1996, 1997, 1998), among the others, investigated the design of a robust controller for reactors described by hyperbolic and parabolic systems of PDE, in presence of a manipulated input and of a controlled output distributed in space: the controller is designed constructively using Lyapunov's direct method and requires that there exist known bounding functions that capture the magnitude of the uncertain terms and a matching condition is satisfied.

The H_∞ control design technique provides an alternative technique to achieve similar results; moreover, this technique involves the design of a state estimator

3

(observer), coupled with the controller (which is a simple state feedback), that guarantees robust performance. In a previous work (Fissore, 2007) a detailed description of this technique has been given, summarising the main results appeared in the Literature and introducing the concept of "extended system" for the control design, where performance requirements and model uncertainty are described. Non-linear variables are linearised around a "nominal" state and the range of values that can be assumed by the non-linear variable is considered as a range of uncertainty around the nominal state.

This is not the only approach that has been proposed in the Literature to account for nonlinearities; recent papers gave extensive results on the control of nonlinear systems that handle uncertainty and constraints: El-Farra & Christofides (2001, 2003) and Mhaskar et al. (2005) focused their attention on the control of multi-input multi-output nonlinear processes with uncertain dynamics and actuator constraints and proposed a Lyapunov-based nonlinear controller design approach that accounts explicitly and simultaneously for process nonlinearities, plant-model mismatch, and input constraints.

This paper is organised in the following way: firstly the process model is given, with all the simplifications required; then the control problem is stated and the "extended model" required for the design of the robust controller (and of the observer) is built up; finally various results proving the effectiveness of the proposed control algorithm are shown.

We would like to highlight that this work is one of the first attempts to apply the H_∞ control technique to a distributed parameters system like a fixed bed reactor; some papers appeared in the past applying this technique to the Chemical Engineering field, but all of them investigated lumped systems like perfectly mixed continuous reactors (see, for example, Galan et al., 2000, and Kolavennu et al., 2000). Even when much more complex systems, like a distillation column, were investigated, simple input-output models were used (Razzaghi and Shahraki, 2007). In this paper we would like to evidence all the potentiality of this method, even at a

vary basic level, but in presence of a detailed model, instead of using a complex theoretically-based H$_\infty$ controller with an elementary model of the process.

Model formulation

The analogy between the countercurrent reactor and the RFR was used in this work to build up a simple model of the process. This analogy was firstly stated by Nieken et al. (1995) and it was demonstrated that it holds when the switching frequency is infinite. Figure 2 shows a sketch of the countercurrent reactor under study. The basic balance equations are given in Appendix 1, with the corresponding boundary conditions.

Normalising some variables and assuming, following Edouard et al. (2004) and for sake of simplicity, that the Nusselt and Sherwood numbers on one hand, and the Schmidt and Prandtl numbers on the other hand, are equal, we obtain the following balance equations for the inert section of the reactor:

$$
\begin{cases}
\tau_{in}\dfrac{\partial T_S}{\partial t} = \dfrac{1}{Pe_{ax,in}}\dfrac{\partial^2 T_{S,in}}{\partial x_{in}^2} + Pe_{in}\left(\dfrac{T_{G,1,in}+T_{G,2,in}}{2}-T_{S,in}\right) \\[2mm]
\alpha\dfrac{\partial T_{G,1,in}}{\partial x_{in}} + Pe_{in}\left(T_{G,1,in}-T_{S,in}\right)=0 \\[2mm]
-\dfrac{\partial T_{G,2,in}}{\partial x_{in}} + Pe_{in}\left(T_{G,2,in}-T_{S,in}\right)=0 \\[2mm]
\dfrac{\partial \omega_{G,1,in}}{\partial x_{in}} = \dfrac{\partial \omega_{G,2,in}}{\partial x_{in}}=0
\end{cases}
\tag{1}
$$

where:

$$
x_{in}=\frac{z}{L_{in}}, \quad \frac{1}{Pe_{ax,in}}=\frac{\lambda_{ax}^S}{\rho_{G,0}v_0 c_{p,G}L_{in}}, \quad \tau_{in}=\frac{(1-\varepsilon)\rho_S c_{p,S}L_{in}}{\rho_{G,0}v_0 c_{p,G}}, \quad Pe_{in}=\frac{h a_v L_{in}}{\rho_{G,0}v_0 c_{p,G}}
\tag{2}
$$

with boundary conditions:

$$\begin{cases} \omega_{G,1,in}\big|_{x_{in}=0} = \omega_{G,0} \\[2mm] \omega_{G,2,in}\big|_{x_{in}=1} = \omega_{G,2,cat}\big|_{x_{cat}=0} \\[2mm] T_{G,1,in}\big|_{x_{in}=0} = T_{G,0} \\[2mm] T_{G,2,in}\big|_{x_{in}=1} = T_{G,2,cat}\big|_{x_{cat}=0} \\[2mm] \dfrac{\partial T_{S,in}}{\partial x_{in}}\bigg|_{x_{in}=0} = 0 \\[4mm] \dfrac{\partial T_{S,in}}{\partial x_{in}}\bigg|_{x_{in}=1} = \dfrac{L_{cat}}{L_{in}}\dfrac{\partial T_{S,cat}}{\partial x_{cat}}\bigg|_{x_{cat}=0} \end{cases} \qquad (3)$$

For the catalytic section of the reactor the contribution of the second reactor to the reaction rate, namely $r_{S,2}$, is assumed to be negligible during normal operation (i.e. far away from reaction extinction) as it was discussed by Fissore et al. (2006). Moreover, mass transfer control is assumed, thus $\omega_{1,S,cat} = 0$; this gives:

$$\begin{cases} \tau_{cat}\dfrac{\partial T_{S,cat}}{\partial t} = \dfrac{1}{Pe_{ax,cat}}\dfrac{\partial^2 T_{S,cat}}{\partial x_{cat}^2} + Pe_{cat}\left(\dfrac{T_{G,1,cat}+T_{G,2,cat}}{2} - T_{S,cat}\right) + \dfrac{a_v(-\Delta H)L_{cat}}{\rho_{G,0}v_0 c_{p,G}}\dfrac{r_{S,1}}{2} \\[4mm] \alpha\dfrac{\partial T_{G,1,cat}}{\partial x_{cat}} + Pe_{cat}\left(T_{G,1,cat}-T_{S,cat}\right) = 0 \\[4mm] -\dfrac{\partial T_{G,2,cat}}{\partial x_{cat}} + Pe_{cat}\left(T_{G,2,cat}-T_{S,cat}\right) = 0 \\[4mm] \alpha\dfrac{\partial \omega_{G,1,cat}}{\partial x_{cat}} + Pe_{cat}\omega_{G,1,cat} = 0 \\[4mm] \dfrac{\partial \omega_{G,2,cat}}{\partial x_{cat}} = 0 \\[4mm] Pe_{cat}\omega_{G,1,cat} = \dfrac{Ma_v L_{cat}}{\rho_{G,0}v_0}r_{S,1} \end{cases} \qquad (4)$$

where:

$$x_{cat} = \dfrac{z}{L_{cat}}, \quad \dfrac{1}{Pe_{ax,cat}} = \dfrac{\lambda_{ax}^S}{\rho_{G,0}v_0 c_{p,G}L_{cat}}, \quad \tau_{cat} = \dfrac{(1-\varepsilon)\rho_S c_{p,S}L_{cat}}{\rho_{G,0}v_0 c_{p,G}}, \quad Pe_{cat} = \dfrac{ha_v L_{cat}}{\rho_{G,0}v_0 c_{p,G}} \qquad (5)$$

$$\begin{cases} \omega_{G,1,cat}\big|_{x_{cat}=0} = \omega_{G,1,in}\big|_{x_{in}=1} \\[2mm] \omega_{G,2,cat}\big|_{x_{cat}=1} = \alpha\,\omega_{G,1,cat}\big|_{x_{cat}=1} \\[2mm] T_{G,1,cat}\big|_{x_{cat}=0} = T_{G,1,in}\big|_{x_{in}=1} \\[2mm] \dfrac{L_{cat}}{L_{in}}\dfrac{\partial T_{S,cat}}{\partial x_{cat}}\bigg|_{x_{cat}=0} = \dfrac{\partial T_{S,in}}{\partial x_{in}}\bigg|_{x_{in}=1} \\[3mm] T_{G,2,cat}\big|_{x_{cat}=1} = \dfrac{\alpha}{(1+N')}T_{G,1,cat}\big|_{x_{cat}=1} + \dfrac{(1+N'-\alpha)}{(1+N')}T_{G,0} + \dfrac{1}{(1+N')\rho_{G,0}v_0 c_{p,G}S}Q_{el} \\[3mm] \dfrac{\partial T_{S,cat}}{\partial x}\bigg|_{x_{cat}=1} = 0 \end{cases} \tag{6}$$

If the assumption that the Nusselt and Sherwood numbers on one hand, and the Schmidt and Prandtl numbers on the other hand, are equal does not hold, the non-dimensional equations describing the dynamics of the system are slightly modified, as it is shown in Appendix 2.

The models given by eq. (1)-(3) for the inert monolith and by eq. (4)-(6) for the catalytic monolith are further simplified using the approach of Balakotaiah and Dommeti (1999), thus expressing the gas temperature as a function of the solid temperature:

$$\begin{cases} T_{G,1} = \left(I + \dfrac{\alpha}{Pe}\dfrac{\partial}{\partial x}\right)^{-1} T_S = T_S + \displaystyle\sum_{k=1}^{\infty}\left(-\dfrac{\alpha}{Pe}\right)^k \dfrac{\partial^k T_S}{\partial x^k} \\[4mm] T_{G,2} = \left(I - \dfrac{1}{Pe}\dfrac{\partial}{\partial x}\right)^{-1} T_S = T_S + \displaystyle\sum_{k=1}^{\infty}\left(\dfrac{1}{Pe}\right)^k \dfrac{\partial^k T_S}{\partial x^k} \end{cases} \tag{7}$$

The convergence of the series is guaranteed when $Pe>1$; as Pe is much greater than unity in this case, it is possible to truncate the development at the second-order term, thus obtaining the following approximations:

$$\begin{cases} T_{G,1} \cong T_S - \dfrac{\alpha}{Pe}\dfrac{\partial T_S}{\partial x} + \left(\dfrac{\alpha}{Pe}\right)^2 \dfrac{\partial^2 T_S}{\partial x^2} \\[4mm] T_{G,2} \cong T_S + \dfrac{1}{Pe}\dfrac{\partial T_S}{\partial x} + \left(\dfrac{1}{Pe}\right)^2 \dfrac{\partial^2 T_S}{\partial x^2} \end{cases} \tag{8}$$

(in eq. (7) and (8) the subscripts "cat" and "in" are omitted). Using eq. (8), the following pseudo-homogeneous heat balance is obtained for the inert monolith:

$$\tau_{in} \frac{\partial T_{S,in}}{\partial t} = \left(\frac{1}{Pe_{ax,in}} + \frac{1+\alpha^2}{2Pe_{in}} \right) \frac{\partial^2 T_{S,in}}{\partial x_{in}^2} + \frac{1-\alpha}{2} \frac{\partial T_{S,in}}{\partial x_{in}} \tag{9}$$

while the pseudo-homogeneous heat balance for the catalytic monolith is:

$$\tau_{cat} \frac{\partial T_{S,cat}}{\partial t} = \left(\frac{1}{Pe_{ax,cat}} + \frac{1+\alpha^2}{2Pe_{cat}} \right) \frac{\partial^2 T_{S,cat}}{\partial x_{cat}^2} + \frac{1-\alpha}{2} \frac{\partial T_{S,cat}}{\partial x_{cat}} + \frac{a_v(-\Delta H)L_{cat}}{\rho_{G,0}v_0 c_{p,G}} \frac{r_{S,1}}{2} \tag{10}$$

$r_{S,1}$ can be calculated using the mass balances thus giving:

$$\tau_{cat} \frac{\partial T_{S,cat}}{\partial t} = \left(\frac{1}{P_{ax,cat}} + \frac{1+\alpha^2}{2Pe_{cat}} \right) \frac{\partial^2 T_{S,cat}}{\partial x_{cat}^2} + \frac{1-\alpha}{2} \frac{\partial T_{S,cat}}{\partial x_{cat}} + Pe_{cat}\Delta T_{ad} \frac{1}{2} e^{-Pe_{cat}\frac{x_{cat}}{\alpha}} \tag{11}$$

where:

$$\Delta T_{ad} = \frac{\omega_{G,0}(-\Delta H)}{Mc_{p,G}} \tag{12}$$

The boundary conditions for the thermal balance equation are modified as now there are no more two gas-phase first-order thermal balance equations and one solid-phase second-order thermal balance equation, but just eq. (9) and (11). As a consequence, the boundary conditions at $x_{in} = 0$ and at $x_{in} = 1$ are obtained writing the energy balance for the pseudo-homogeneous system (solid+gas) and expressing the gas temperature as a function of the solid temperature according to eq. (8):

$$\begin{cases} T_{S,in}\big|_{x_{in}=0} - \frac{\alpha}{Pe_{in}}\frac{\partial T_{S,in}}{\partial x_{in}}\bigg|_{x_{in}=0} = T_{G,0} \\ T_{S,in}\big|_{x_{in}=1} = T_{S,cat}\big|_{x_{cat}=0} \\ \frac{\partial T_{S,in}}{\partial x_{in}}\bigg|_{x_{in}=1} = \frac{L_{cat}}{L_{in}}\frac{\partial T_{S,cat}}{\partial x_{cat}}\bigg|_{x_{cat}=0} \end{cases} \tag{13}$$

Similarly, for the catalytic monolith the boundary conditions are now:

$$\begin{cases} T_{S,cat}\big|_{x_{cat}=0} = T_{S,in}\big|_{x_{in}=1} \\ \frac{L_{cat}}{L_{in}}\frac{\partial T_{S,cat}}{\partial x_{cat}}\bigg|_{x_{cat}=0} = \frac{\partial T_{S,in}}{\partial x_{in}}\bigg|_{x_{in}=1} \\ T_S\big|_{x_{cat}=1} = \left\{ \frac{-1-N'-\alpha^2}{Pe_{cat}(1+N'-\alpha)} \right\} \frac{\partial T_S}{\partial x}\bigg|_{x_{cat}=1} + T_{G,0} + \frac{1}{(1+N'-\alpha)\rho_{G,0}v_0 c_{p,G}S}Q_{el} \end{cases} \tag{14}$$

As we have distinguished between the balances of the inert and of the catalytic solid,

we are sure that whatever is the space discretisation used, the temperature at the interface between the two solids is calculated; this is of paramount importance as this temperature is the controlled variable of the process as it will be demonstrated in the next paragraphs.

The finite frequency in the RFR is responsible for a deviation with respect to the prediction based on the countercurrent model; the simple correction introduced by Edouard et al. (2004) is used to take into account the finite flow reversal frequency.

The numerical solution of the problem has been carried out by discretising the spatial domains of the system, thus transforming the PDE (9)-(11) (with boundary conditions given by eq. (13)-(14)) into an ODE system. The orthogonal collocations method has been adopted in order to find the solution in the nodes of the discretised domain: the unknown solution of a differential equation is expanded as a global interpolant, such as a trigonometric or polynomial function (a comprehensive description can be found in various books and papers, see for example Canuto et al., 1988, Funaro, 1992, and Fornberg, 1996):

$$f(x) \cong \sum_{j=0}^{n+1} f\left(x_j\right) l_j(x) \tag{15}$$

where x_0 and x_{n+1} are the points where the boundary conditions are defined, $\left\{x_j\right\}$ is a set of n distinct interpolation nodes and l_j are the Lagrangian interpolating polynomials of degree n satisfying the condition:

$$l_j\left(x_i\right) = \delta_{ij} \tag{16}$$

and thus defined by:

$$l_j(x) = \prod_{i=1, i \neq j}^{n} \frac{x - x_i}{x_j - x_i} \tag{17}$$

The best choice for the interpolation nodes are the roots of orthogonal polynomials such as the Jacobi, Laguerre, and Hermite polynomials. In this case, as the points x_0 and x_{n+1} are involved in the calculation, the best choice for the points $\left\{x_j\right\}$ is given by the zeroes of the polynomial of Jacobi $P_n^{\alpha,\beta}(x)$ with $\alpha = \beta = 1$, defined over the

interval [0, 1].

If we consider the solution of eq. (9) the approximated solution is:

$$T_{S,in}(t,x) \cong \sum_{j=0}^{n_{in}+1} T_{S,in}(t,x_{j,in}) l_{j,in}(x) \tag{18}$$

where n_{in} is the number of collocation points in the inert monolith, thus:

$$\begin{cases} \dfrac{dT_{S,in}(t,x)}{dx} = \displaystyle\sum_{j=0}^{n_{in}+1} T_{S,in}(t,x_{j,in}) l_{j,in}^{(1)}(x) \\[4mm] \dfrac{d^2 T_{S,in}(t,x)}{dx^2} = \displaystyle\sum_{j=0}^{n_{in}+1} T_{S,in}(t,x_{j,in}) l_{j,in}^{(2)}(x) \end{cases} \tag{19}$$

Eq. (18) and (19) are then introduced in eq. (9), thus resulting in the collocation points:

$$\frac{\partial T_{S,in}(t,x_{i,in})}{\partial t} = \frac{1}{\tau_{in}} \left(\frac{1}{Pe_{ax,in}} + \frac{1+\alpha^2}{2Pe_{in}} \right) \left[\sum_{j=0}^{n_{in}+1} T_{S,in}(t,x_{j,in}) l_{j,in}^{(2)}(x_{i,in}) \right] +$$
$$+ \frac{1-\alpha}{2\tau_{in}} \left[\sum_{j=0}^{n_{in}+1} T_{S,in}(t,x_{j,in}) l_{j,in}^{(1)}(x_{i,in}) \right] \tag{20}$$

with boundary conditions:

$$\begin{cases} \left[\displaystyle\sum_{j=0}^{n_{in}+1} T_{S,in}(t,x_{j,in}) l_{j,in}(x_{0,in}) \right] - \dfrac{\alpha}{Pe_{in}} \left[\displaystyle\sum_{j=0}^{n_{in}+1} T_{S,in}(t,x_{j,in}) l_{j,in}^{(1)}(x_{0,in}) \right] = T_{G,0} \\[5mm] \left[\displaystyle\sum_{j=0}^{n_{in}+1} T_{S,in}(t,x_{j,in}) l_{j,in}(x_{n_{in}+1,in}) \right] = \left[\displaystyle\sum_{j=0}^{n_{cat}+1} T_{S,cat}(t,x_{j,cat}) l_{j,cat}(x_{0,cat}) \right] \\[5mm] \left[\displaystyle\sum_{j=0}^{n_{in}+1} T_{S,in}(t,x_{j,in}) l_{j,in}^{(1)}(x_{n_{in}+1,in}) \right] = \dfrac{L_{cat}}{L_{in}} \left[\displaystyle\sum_{j=0}^{n_{cat}+1} T_{S,cat}(t,x_{j,cat}) l_{j,cat}^{(1)}(x_{0,cat}) \right] \end{cases} \tag{21}$$

If we consider the solution of eq. (11) in a certain time instant the approximated solution is:

$$T_{S,cat}(t,x) \cong \sum_{j=0}^{n_{cat}+1} T_{S,cat}(t,x_{j,cat}) l_{j,cat}(x) \tag{22}$$

where n_{cat} is the number of collocation points in the catalytic monolith, thus:

$$\begin{cases} \dfrac{dT_{S,cat}(t,x)}{dx} = \displaystyle\sum_{j=0}^{n_{cat}+1} T_{S,cat}(t,x_{j,cat}) l_{j,cat}^{(1)}(x) \\[4mm] \dfrac{d^2 T_{S,cat}(t,x)}{dx^2} = \displaystyle\sum_{j=0}^{n_{in}+1} T_{S,cat}(t,x_{j,cat}) l_{j,cat}^{(2)}(x) \end{cases} \tag{23}$$

Eq. (22) and (23) are then introduced in eq. (11), thus resulting in:

$$\frac{\partial T_{S,cat}(t,x_{i,cat})}{\partial t} = \frac{1}{\tau_{cat}}\left(\frac{1}{Pe_{ax,cat}}+\frac{1+\alpha^2}{2Pe_{cat}}\right)\left[\sum_{j=0}^{n_{cat}+1}T_{S,cat}(t,x_{j,cat})l_{j,cat}^{(2)}(x_{i,cat})\right]+$$

$$+\frac{1-\alpha}{2\tau_{cat}}\left[\sum_{j=0}^{n_{cat}+1}T_{S,cat}(t,x_{j,cat})l_{j,cat}^{(1)}(x_{i,cat})\right]+\frac{Pe_{cat}}{2\tau_{cat}}e^{-Pe_{cat}\frac{x_{i,cat}}{\alpha}}\Delta T_{ad}$$

(24)

with boundary conditions:

$$\begin{cases}\left[\sum_{j=0}^{n_{cat}+1}T_{S,cat}(t,x_{j,cat})l_{j,cat}(x_{0,cat})\right]=\left[\sum_{j=0}^{n_{in}+1}T_{S,in}(t,x_{j,in})l_{j,in}(x_{n_{in}+1,in})\right]\\[2em]\frac{L_{cat}}{L_{in}}\left[\sum_{j=0}^{n_{cat}+1}T_{S,cat}(t,x_{j,cat})l_{j,cat}^{(1)}(x_{0,cat})\right]=\left[\sum_{j=0}^{n_{in}+1}T_{S,in}(t,x_{j,in})l_{j,in}^{(1)}(x_{n_{in}+1,in})\right]\\[2em]\left[\sum_{j=0}^{n_{cat}+1}T_{S,cat}(t,x_{j,cat})l_{j,cat}(x_{n_{cat}+1,cat})\right]=\left\{\frac{-1-N'-\alpha^2}{Pe_{cat}(1+N'-\alpha)}\right\}\left[\sum_{j=0}^{n_{cat}+1}T_{S,cat}(t,x_{j,cat})l_{j,cat}^{(1)}(x_{n_{cat}+1,cat})\right]+\\[2em]\qquad\qquad\qquad +T_{G,0}+\frac{1}{(1+N'-\alpha)\rho_{G,0}v_0c_{p,G}S}Q_{el}\end{cases}$$

(25)

If we organise the first ($l^{(1)}$) and the second ($l^{(2)}$) order derivatives of the Lagrangian polynomial in the differentiation matrix D^1 and D^2 defined as:

$$D_{i,j,in}^1=l_{j,in}^{(1)}(x_{i,in}),D_{i,j,cat}^1=l_{j,cat}^{(1)}(x_{i,cat}),D_{i,j,in}^2=l_{j,in}^{(2)}(x_{i,in}),D_{i,j,cat}^2=l_{j,cat}^{(2)}(x_{i,cat})$$

(26)

and re-define some variables, eq. (20) and (21) can be written as:

$$\begin{cases}\frac{\partial y_{i,in}}{\partial t}=a_{in}\sum_{j=0}^{n_{in}+1}D_{i,j,in}^2y_{j,in}+b_{in}\sum_{j=0}^{n_{in}+1}D_{i,j,in}^1y_{j,in}\\[1.5em]y_{0,in}-\frac{\alpha}{P_{in}}\sum_{j=0}^{n_{in}+1}D_{0,j,in}^1y_{j,in}=T_{G,0}\\[1.5em]y_{n_{in}+1,in}=y_{0,cat}\\[1.5em]\sum_{j=0}^{n_{in}+1}D_{n_{in}+1,j,in}^1y_{j,in}=\frac{L_{cat}}{L_{in}}\sum_{j=0}^{n_{cat}+1}D_{0,j,cat}^1y_{j,cat}\end{cases}$$

(27)

with:

$$a_{in}=\frac{1}{\tau_{in}}\left(\frac{1}{Pe_{ax,in}}+\frac{1+\alpha^2}{2Pe_{in}}\right),\ b_{in}=\frac{1}{\tau_{in}}\frac{1-\alpha}{2},\ y_{j,in}=T_{S,in}(t,x_{j,in})$$

(28)

while eq. (24) and (25) give:

$$\begin{cases} \dfrac{\partial y_{i,cat}}{\partial t} = a_{cat} \sum_{j=0}^{n_{cat}+1} D^2_{i,j,cat} y_{j,cat} + b_{cat} \sum_{j=0}^{n_{cat}+1} D^1_{i,j,cat} y_{j,cat} + \dfrac{Pe_{cat}}{2\tau_{cat}} e^{-Pe_{cat}\frac{x_{i,cat}}{\alpha}} \Delta T_{ad} \\[2ex] y_{0,cat} = y_{n_{in}+1,in} \\[2ex] \dfrac{L_{cat}}{L_{in}} \sum_{j=0}^{n_{cat}+1} D^1_{0,j,cat} y_{j,cat} = \sum_{j=0}^{n_{in}+1} D^1_{n_{in}+1,j,in} y_{j,in} \\[2ex] y_{n_{cat}+1,cat} = c_{cat} \sum_{j=0}^{n_{cat}+1} D^1_{n_{cat}+1,j,cat} y_{j,cat} + T_{G,0} + \dfrac{1}{(1+N'-\alpha)\rho_{G,0} v_0 c_{p,G} S} Q_{el} \end{cases} \qquad (29)$$

with:

$$a_{cat} = \frac{1}{\tau_{cat}} \left(\frac{1}{Pe_{ax,cat}} + \frac{1+\alpha^2}{2Pe_{cat}} \right), \ b_{cat} = \frac{1}{\tau_{cat}} \frac{1-\alpha}{2}, \ c_{cat} = \left\{ \frac{-1-N'-\alpha^2}{Pe_{cat}(1+N'-\alpha)} \right\}, \ y_{j,cat} = T_{S,cat}\left(t, x_{j,cat}\right) \qquad (30)$$

After some algebraic manipulations, the equations describing the time evolution of the temperature of the solid temperature are given by:

$$\frac{dT_S}{dt} = A(\alpha) T_S + B_1(\alpha) T_{G,0} + B_2(\alpha) Q_{el} + E(\alpha) \Delta T_{ad} \qquad (31)$$

where:

$$T_S = \begin{bmatrix} T_{S,in} \\ T_{S,cat} \end{bmatrix}, T_{S,in} = \begin{bmatrix} T_{S,in}\left(x_{1,in}\right) \\ \vdots \\ T_{S,in}\left(x_{1,n_{in}}\right) \end{bmatrix}, T_{S,cat} = \begin{bmatrix} T_{S,cat}\left(x_{1,cat}\right) \\ \vdots \\ T_{S,cat}\left(x_{1,n_{cat}}\right) \end{bmatrix} \qquad (32)$$

Appendix 3 gives the values of the matrices $A(\alpha), B_1(\alpha), B_2(\alpha), E(\alpha)$.

Design of the controller

It has been stated in the Introduction that the control system is required to avoid the extinction of the combustion reaction and the overheating of the catalyst when the feeding concentration changes. If the feed concentration results in a temperature profiles that allows for complete pollutant conversion without damaging the catalysts, no control action is required: neither the electric heating (Q_{el}) nor the fresh air dilution (α) are active. If the pollutant concentration of the feed is too low to

12

ensure full conversion, electric heating is required; however, the heating power should be kept as small as possible to reduce the cost. On the contrary, if the concentration of the feed is so high that the maximum allowable temperature of the catalyst is overcome, fresh air is introduced in the reactor. Therefore, the reactor works at the upper limit temperature in dilution phase, when the feed of pollutant concentration is rich, and at the lower limit temperature in heating phase, when the feed is lean. Heating and cooling together must be avoided. Consequently, two controllers are required: one in presence of rich feed, which uses air dilution as manipulated variable, and the other in presence of lean feed, using electric heating as manipulated variable. According to the temperature measurements, both controllers may be deactivated, or one specific can be active.

The key question is the choice of the "upper" and of the "lower" limit temperature profiles; most of the reaction takes place at the inlet of the catalytic monolith and is instantaneous (Nieken et al., 1995; Ramdani et al., 2001). Therefore, instead of the full temperature profile, only the temperature at the entrance of the catalytic section $T_S(x_{cat,0})$ has to be controlled. For the case study under investigation the minimal temperature $T_S(x_{cat,0})$ required to ensure full conversion and the maximum temperature to avoid overheating of the catalytic monolith are respectively 450 and 600 K. Thus, if $T_S(x_{cat,0})$ is between the two limit values no control action is required, while if it overcomes 600 K, dilution is required to avoid catalyst overheating and if it becomes lower than 450 K, electrical heating is required.

Robust control technique described in detail by Fissore (2007) is used to design the two controllers; this technique applies to linear systems, thus we need first to linearise the model (31) around the nominal steady-states for the two controllers:

1. For the calculation of the steady-state profile corresponding to the "lower" limit (indicated with the superscript "0") we assume that $\Delta T_{ad}^0 = 0$ K; with dilution kept as low as it is possible ($\alpha^0 = 0.95$, due to leakage), the limit temperature $T_S^0\left(x_{cat,0}\right)=$ 450 K is maintained with $Q_{el}^0 = 1100$ W (with a feed flow rate of 100 Nm³ h⁻¹); the

corresponding temperature steady-state profile is Z^0.

2. For the calculation of the steady-state profile corresponding to the "upper" limit (indicated with the superscript "1") we assume that the maximum feeding concentration corresponds to $\Delta T_{ad}^1 = 100$ K; in this case no external heating is required, thus $Q_{el}^1 = 0$ W, and the limit temperature $T_S^1(x_{cat,0}) = 600$ K is maintained with a dilution resulting in $\alpha^1 = 0.75$; the corresponding temperature steady-state profile is Z^1.

It is important to highlight that the control actions corresponding to the two limiting steady-state, i.e. Q_{el}^0 and α^1, are calculated assuming that the feeding concentration can have a ΔT_{ad} variable in the range 0 and 100 K; if this range is different, the values of external heating and of dilution corresponding to the two limiting steady-state will be different.

The balance equation system (31) can be linearised around the generic steady state Z^j, resulting in:

$$\Delta \dot{T}_S(t) = A(\alpha^j)\Delta T_S(t) +$$
$$+ \left\{ \frac{\partial A(\alpha)}{\partial \alpha}\bigg|_{\alpha^j} Z^j + \frac{\partial B_1(\alpha)}{\partial \alpha}\bigg|_{\alpha^j} T_0^j + \frac{\partial B_2(\alpha)}{\partial \alpha}\bigg|_{\alpha^j} Q_{el}^j + \frac{\partial E(\alpha)}{\partial \alpha}\bigg|_{\alpha^j} \Delta T_{ad}^j \right\}\Delta \alpha + \tag{33}$$
$$+ B_2(\alpha^j)\Delta Q_{el} + E(\alpha^j)\Delta(\Delta T_{ad}(t))$$

where $\Delta T_S = T_S - Z^j$, $\Delta \alpha = \alpha - \alpha^j$, $\Delta Q_{el} = Q_{el} - Q_{el}^j$; $\Delta(\Delta T_{ad})$ plays the role of disturbance. Thus, if we are approaching extinction, the linearised model describing the dynamics of the system is:

$$\Delta \dot{T}_S(t) = A(\alpha^0)\Delta T_S(t) + B_2(\alpha^0)\Delta Q_{el} + E(\alpha^0)\Delta(\Delta T_{ad}(t)) \tag{34}$$

while if we are approaching catalyst overheating, the linearised model describing the dynamics of the system is:

$$\Delta \dot{T}_S(t) = A(\alpha^1)\Delta T_S(t) +$$
$$+ \left\{ \frac{\partial A(\alpha)}{\partial \alpha}\bigg|_{\alpha^1} Z^1 + \frac{\partial B_1(\alpha)}{\partial \alpha}\bigg|_{\alpha^1} T_0^1 + \frac{\partial B_2(\alpha)}{\partial \alpha}\bigg|_{\alpha^1} Q_{el}^1 + \frac{\partial E(\alpha)}{\partial \alpha}\bigg|_{\alpha^1} \Delta T_{ad}^1 \right\}\Delta \alpha + \tag{35}$$
$$+ E(\alpha^1)\Delta(\Delta T_{ad}(t))$$

Eq. (34) and (35) are two linear models that can be used to design the two linear robust controllers.

Control system design to avoid reaction extinction

Figure 3 (upper graph) shows a block diagram corresponding to eq. (34); the block $C(\alpha^0)$ corresponds to a matrix that allows extracting from the array ΔT_S the controlled (and measured) states: we assume to measure the temperatures at the entrance of the inert monolith (ΔT_1) and at the boundaries of the catalytic monolith (ΔT_2 and ΔT_3), while the controlled variable is the temperature at the interface between the inert and the catalytic monolith (ΔT_2). Obviously we measure T_1, T_2 and T_3 and not ΔT_1, ΔT_2 and ΔT_3, but, as Z^0 is known, from the measure of the temperatures it is possible to calculate the difference of these temperatures from the desired steady-state.

Roughly speaking, the control system will act when the reaction is approaching extinction in order to maintain the system at the state Z^0, i.e. to guarantee insensitivity of ΔT_2 with respect to disturbances $\Delta(\Delta T_{ad})$ (i.e. to maintain the temperature at the interface inert-catalytic monolith at the steady-state value) acting on the ΔQ_{el} (i.e. varying Q_{el} from the steady-state value of 1100 W) with a full-state feedback, i.e.:

$$\Delta Q_{el} = -K^0 \Delta T_S \tag{36}$$

The whole temperature profile is required to calculate the control action, as the controller is a full state feedback.

For the calculation of the controller gain K^0 we need to specify the performance requirements:

1. process performance: $\Delta T_{S,2}$ should be kept as small as possible; in our analysis we assumed a performance filter $W_{w,zT} = 10$, thus requiring a sensitivity between the disturbance and the controlled variable lower than 0.1 for all the frequencies;

2. control activity: as the control action is based on the measurements and they

can be affected by noise (n_1, n_2 and n_3 for the three temperatures measured), we require a low sensitivity of the control action with respect to these noises and we assume performance filters $W_{n_1,u} = W_{n_2,u} = W_{n_2,u} = 10$.

Beside the performance requirements, we need to specify the robust performance required, i.e. the range of the values of the parameters of the model. For this application uncertainties are due to:

i. modelling hypothesis: the countercurrent reactor is a good approximation of the RFR only when the switching frequency is infinite; moreover, mass transfer control is assumed and the gas temperature is assumed to be a function of the solid temperature according to eq. (8);

ii. model linearisation around the desired steady-state;

iii. parameter calculation (transport coefficients, physical properties of the gas and of the monoliths).

The result is that the coefficients of the matrices $A(\alpha^0)$, $B_2(\alpha^0)$, $E(\alpha^0)$ and $C(\alpha^0)$ can vary in a certain range. We assume that:

$$\begin{cases} A(\alpha^0) = A(I + \Delta^* W_A) \\ B_2(\alpha^0) = B_2(I + \Delta^* W_{B_2}) \\ C(\alpha^0) = C(I + \Delta^* W_C) \\ E(\alpha^0) = E(I + \Delta^* W_E) \end{cases} \tag{37}$$

where A, B_2, C and E are the nominal values of the matrices of the system, I is a matrix (of adequate dimension) whose coefficients are equal to 1, Δ^* is a matrix whose norm H_∞ is lower than 1 and W_A, W_{B2}, W_C and W_E are the filters specifying the variability of the matrices.

Assuming that the physical properties of the system, the geometrical dimensions and the state around which the linearisation is made (i.e. the target value of the temperature profile) are well known, we have to make hypothesis about the sources of uncertainty in order to determine the range of variability of these matrices. We have stated in the paragraph describing the model, that a correction for the finite

flow reversal frequency was included in the model (see Edouard et al., 2004); it consists of a modification of the parameters Pe and Pe_{ax} (both for the catalytic and for the inert section of the reactor), which thus represent the main source of uncertainty of all the matrices. It must be considered that in the definition of these two parameters both the heat transfer coefficient and the solid thermal conductivity, which can be poorly known (see Appendix 3), appear. If we assume a variation of the two parameters of ±10% around their nominal values, the coefficients of the matrices A, B_2, C and E can be calculated in the two limit cases and they show a maximum variation around their nominal values of about ±10%: for sake of simplicity the coefficients of the filters are set equal to 0.1. The other source of uncertainty is the state around which the system is linearised; anyway, this state can be regarded as a target value that should be maintained when the system is approaching extinction and so it is fixed by the user. The control system does not operate when the system is far from extinction: it has been stated that it acts only when the maximum (monitored) temperature falls below a lower limit; in this condition the linearised model is adequate to describe the dynamics of the reactor.

The results of this specifications is the "extended model" shown in Figure 3 (lower graph); various couples of input-output signals emerge:

1. $\Delta(\Delta T_{ad})$-z_T represents the channel disturbance-objectives ($W_{w,zT}$ is the corresponding performance filter);

2. n_1-z_{n1} represents the channel measurement noise on the first temperature (T_1)-control activity (the performance filter is $W_{n1,u}$)

3. n_2-z_{n2} represents the channel measurement noise on the second temperature (T_2)-control activity (the performance filter is $W_{n2,u}$)

4. n_3-z_{n3} represents the channel measurement noise on the third temperature (T_3)-control activity (the performance filter is $W_{n3,u}$)

5. w_A-z_A represents the uncertainty channel due to A;

6. w_{B2}-z_{B2} represents the uncertainty channel due to B_2;

7. w_C-z_C represents the uncertainty channel due to C;

8. w_E-z_E represents the uncertainty channel due to E;

The extended system defines a multivariable operator GW with inputs

$$w = \left\{ \Delta\left(\Delta T_{ad}\right), n_1, n_2, n_3, w_A, w_{B2}, w_C, w_E \right\} \tag{38}$$

and outputs:

$$z = \left\{ z_T, z_{n_1}, z_{n_2}, z_{n_2}, z_A, z_{B2}, z_C, z_E \right\} \tag{39}$$

If all the states of the system (i.e. the values of ΔT_S) are measured, robust performance (i.e. the desired performance in all the uncertainty range) is obtained if it is possible to find a controller gain K^0 such that the H_∞ norm of all the channels input-output of the multivariable operator GW is lower than zero. More details about the theoretical foundation of this result and about the details of the calculus can be found in Fissore (2007).

As only three temperatures are measured (or better, three differences between the temperature and the desired steady-state values) an observer is required to get the estimation of the other states and to guarantee robust performance, i.e the optimum observer in the worst disturbance condition has to be calculated. The procedure described by Fissore (2007) was followed, and thus no further details are given here. An example of the results obtained with the system observer+controller is given in Figure 4: the reactor is considered to be at the steady-state Z^0 at t=0, when the inlet concentration (i.e. the ΔT_{ad}) is changed; the time evolution of ΔT_2 (i.e. the difference between the actual value of T_2 and its set point) is shown, together with the calculated control action (given as variation of Q_{el} from the steady-state value of 1100 W). Fast and accurate regulation (according to the requested performance) is obtained with the calculated controller; moreover, some tests have been made changing the values of the coefficients of the matrices A, B_2, C and E within the range of uncertainty assumed around the nominal value and again the calculated controller showed good results (which are analogous to those of Figure 4 and thus are not shown here for brevity).

Control system design to avoid catalyst overheating

The design of the control system to avoid catalyst overheating, acting on the dilution, follows the same steps described in the previous paragraph about the control of the extinction of the reaction. The block diagram corresponding to eq. (35) is similar to that shown in Figure 3 for eq. (34): the only difference is that now the manipulated variable is the dilution ($\Delta\alpha$) and no more the electric heating (now in fact $Q_{el} = 0$). Obviously the matrices $A(\alpha^0)$, $E(\alpha^0)$ and $C(\alpha^0)$ are now replaced by $A(\alpha^1)$, $E(\alpha^1)$ and $C(\alpha^1)$, while the matrix $B_2(\alpha^0)$ is replaced by

$$B_2^1(\alpha^1) = \left\{ \left.\frac{\partial A(\alpha)}{\partial \alpha}\right|_{\alpha^1} Z^1 + \left.\frac{\partial B_1(\alpha)}{\partial \alpha}\right|_{\alpha^1} T_0^1 + \left.\frac{\partial B_2(\alpha)}{\partial \alpha}\right|_{\alpha^1} Q_{el}^1 + \left.\frac{\partial E(\alpha)}{\partial \alpha}\right|_{\alpha^1} \Delta T_{ad}^1 \right\} \tag{40}$$

The same measured variables are used in the control loop, aiming to guarantee insensitivity of ΔT_2 with respect to disturbances $\Delta(\Delta T_{ad})$ (i.e. to maintain the temperature at the interface inert-catalytic monolith at the steady-state value) acting on the $\Delta\alpha$ (i.e. varying α from the steady-state value of 0.75) with a full-state feedback, i.e.:

$$\Delta\alpha = -K^1 \Delta T_S \tag{41}$$

Again all the temperature profile is required to calculate the control action. For the calculation of the controller gain K^1 the same requirements on the regulation and on the control activity previously posed are used, as well as the same range for the coefficients of the matrices, thus taking into account model uncertainties.

Again, following the detailed procedure outlined by Fissore (2007) both the observer and the controller satisfying the condition on the norm of the multivariable operator arising from the extended model have been calculated. An example of the results obtained with the system observer+controller is given in Figure 5: the reactor is considered to be at the steady-state Z^1 at $t=0$, when the inlet concentration is changed; the time evolution of ΔT_2 (i.e. the difference between the actual value of T_2 and its set point) is shown, together with the calculated control action (given as variation of α from the steady-state value of 0.95). Fast and accurate regulation

(according to the requested performance) is obtained with the calculated controller; moreover, some tests have been made changing the values of the coefficients of the matrices of the system within the range ±10% around the nominal value and again the calculated controller showed good results (which are analogous to those of Figure 5 and thus are not shown here for brevity).

Controller validation

A final test was made to verify the effectiveness of the proposed control system. The reactor is assumed to be initially at the steady-state Z^0 and the feed concentration, given as ΔT_{ad}, is assumed to vary randomly between 20°C and 40°C. The control action is calculated according to eq. (36) or eq. (41) as a function of the temperature T_2. When the temperature at the inert-catalyst interface is in the allowed range, no control action is undertaken and the value of dilution α or of electrical heating Q_{el} is not changed. Figure 6 shows the values of the input (both disturbances and manipulated variables) of the system as well as the controlled temperature, which is maintained in the desired range. Figure 7 shows the time evolution of the spatial temperature profile, showing the effectiveness of the proposed control system in maintaining the reactor ignited, beside avoiding catalyst overheating.

Conclusions

In conclusion, we would like to summarise the advantages of the proposed method:
- first of all, it is very easy to implement control laws like those of eq. (36) or (41) as they are just state feedback;
- secondly, as the full state of the system is not measured but is required to calculate the control action, an observer is required to know all the states; moreover the observer must be designed for the worst case disturbance in order to guarantee the performance of the control system and its robustness;

- moreover, the control system is designed to ensure a well defined performance in a well defined uncertainty interval: if the norm H_∞ of the "extended model" comprising performance and uncertainties is lower than 1 the robust performance are guaranteed, otherwise the detailed exam of the norm of the various input-output channels of the operator indicates if the uncertainty interval is too large or if the performance requirements are too tight, thus guiding the design of the control system.

Acknowledgement

Notation

a_{in}, b_{in}	Non dimensional parameters defined in eq. (28)
a_{cat}, b_{cat}, c_{cat}	Non dimensional parameters defined in eq. (30)
a_v	Specific surface area of the solid, m² m⁻³
c_p	Specific heat, J kg⁻¹K⁻¹
D^1, D^2	Differentiation matrix
h	Heat transfer coefficient between the gas and the solid, J s⁻¹m⁻²K⁻¹
k_D	Mass transfer coefficient between the gas and the solid, m s⁻¹
K	Controller gain
l_j	Lagrangian interpolating polynomial in the point x_j
L	Length of a monolith, m
M	Molecular mass of the feed, kg mol⁻¹
n	Measurement noise
N'	Number of transfer units for heat loss
Pe	Peclet number for gas-solid heat transfer
Pe_{ax}	Axial Peclet number for heat conduction
$P_n^{\alpha,\beta}$	Polynomial of Jacoby of degree n
Q_{el}	External power supply, J s⁻¹
r_S	Reaction rate, mol m⁻¹s⁻¹
S	Cross section of the monolith, m²
t	Time, s
T	Temperature, K
v	Surface gas velocity, m s⁻¹
W	Performance filter
x	Non-dimensional axial coordinate
y	Solid temperature evaluated in the collocation point, K

| z | Axial coordinate, m |
| Z | Steady-state temperature profile used for linearisation |

Greeks

α	Fraction of the feed flow rate
δ_{ij}	Function of Kronecker
Δ	Variation from the steady-state value
Δ^*	Bounded operator with norm H_∞ lower than 1
$-\Delta H$	Heat of reaction, J mol^{-1}
ΔT_{ad}	Adiabatic temperature rise of the feed, K
ε	Solid void fraction
λ_{ax}^{S}	Axial thermal conductivity of the solid, J s^{-1}m^{-1}K^{-1}
ρ	Density, kg m^{-3}
τ	Time constant for heat storage, s
ω	Mass fraction

Subscripts

0	Feeding value
1, 2	Indicate the first and the second half of the reactor
cat	Catalytic monolith
G	Gas phase
in	Inert monolith
S	Solid phase

Superscripts

| 0 | Refers to the lower temperature operating limit |
| 1 | Refers to the higher temperature operating limit |

Abbreviations

PDE	Partial Differential Equations
RFR	Reverse Flow Reactor
VOC	Volatile Organic Compound

References

Balakotaiah, V., Dommeti, S. M. S. (1999). Effective models for packed-bed catalytic reactors. Chemical Engineering Science, 54, 1621-1638.

Barresi, A. A., Vanni, M. (2002a). Dynamics and control of forced-unsteady-state catalytic combustors, in "*Nonlinear dynamics and control in process engineering – Recent advances*" (G. Continillo, S. Crescitelli & M. Giona, Eds.). Springer-Verlag, Milano, pp. 73-88.

Barresi, A. A., Vanni, M. (2002b). Control of catalytic combustors with periodical flow reversal. AIChE Journal, 48, 648-652.

Canuto, C., Hussaini, M. Y., Quarteroni, A., Zang, T.A. (1988). Spectral methods in fluid dynamics. Springer-Verlag, Berlin.

Christofides, P. D., Daoutidis, P. (1996). Feedback control of hyperbolic PDE systems, AIChE Journal, 42, 3063-3086.

Christofides, P. D., Daoutidis P. (1997). Finite-dimensional control of parabolic PDE systems using approximate inertial manifolds. Journal of Mathematical Analysis and Applications, 216, 398-420.

Christofides, P. D. , Daoutidis, P. (1998). Robust control of hyperbolic PDE systems. Chemical Engineering Science, 53, 85-105.

Edouard, D., Schweich, D., Hammouri, H. (2004). Observer design for reverse flow reactor. AIChE Journal, 50, 2155-2166.

Edouard, D., Hammouri, H., Zhou, X. G. (2005a). Control of a reverse flow reactor for VOC combustion. Chemical Engineering Science, 60, 1661-1672.

Edouard, D., Dufour, P., Hammouri, H. (2005b). Observer based multivariable control of a catalytic reverse flow reactor: comparison between LQR and MPC approaches. Computers and Chemical Engineering, 29, 851-865.

El-Farra, N., Christofides, P. D. (2001). Integrating robustness, optimality and

constraints in control of nonlinear processes. Chemical Engineering Science, 58, 1841-1868.

El-Farra, N., Christofides, P. D. (2003). Bounded robust control of constrained multivariable nonlinear processes. Chemical Engineering Science, 58, 3025-3047.

Fissore, D., Edouard, D., Hammouri, H., Barresi, A. A. (2006). Non-linear soft-sensors design for unsteady-state VOC afterburners. AIChE Journal, 52, 282-291.

Fissore, D. (2007). Robust control of nonlinear processes with uncertainties: observer based state feedback design. Chemical Engineering Science, submitted.

Fornberg, B. (1996). A practical guide to pseudospectral methods. Cambridge University Press, Cambridge.

Funaro, D. (1992). Polynomial approximation of differential equations. Springer-Verlag, Berlin.

Galan, O., Romagnoli, J. A., Palazoglu, A. (2000). Robust H_∞ control of nonlinear plants based on multi-linear models: an application to a bench scale pH neutralisation reactor, Chemical Engineering Science, 55, 4435-4450.

Hevia, M. A. G., Ordóñez, S., Díez, F. V., Fissore, D., Barresi, A. A. (2005). Design and testing of a control system for reverse-flow catalytic afterburners. AIChE Journal, 51, 3020-3027.

Kolavennu, S., Palanki, S., Cockburn, J. C. (2000). Robust control of I/O linearizable systems via multi-model H_2/H_∞ synthesis. Chemical Engineering Science, 55, 1583-1589.

Kolios, G., Frauhammer, J., Eigenberger, G. (2000). Authothermal fixed bed reactor concepts. Chemical Engineering Science, 55, 5945-5967.

Matros, Y. H., Bunimovich, G. A. (1996). Reverse flow operation in fixed bed

catalytic reactors. Catalysis Review-Science and Engineering, 38, 1-68.

Mhaskar, P., El-Farra, N., Christofides, P. D. (2005). Robust hybrid predictive control of nonlinear systems. Automatica, 41, 209-217.

Nieken, U., Kolios, G., Eigenberger, G. (1995). Limiting cases and approximate solutions for fixed-bed reactors with periodic flow reversal. AIChE Journal, 48, 191 –1925.

Ramdani, K., Pontier, R., Schweich, D. (2001). Reverse flow reactor at short switching period for VOC combustion. Chemical Engineering Science, 56, 1531-1539.

Razzaghi, K., Shahraki F. (2007). Robust control of an ill-conditioned plant using μ-synthesis: a case study for high-purity distillation. Chemical Engineering Science, 62, 1543-1547.

Appendix 1

The basic balance equations for the countercurrent reactor are:

$$\lambda_{ax}^S \frac{\partial^2 T_S}{\partial z^2} + \frac{ha_v}{2}\left(T_{G,1} - T_S\right) + \frac{ha_v}{2}\left(T_{G,2} - T_S\right) + a_v\left(-\Delta H\right)\frac{r_{S,1} + r_{S,2}}{2}\varphi(z) = \left(1 - \varepsilon\right)\rho_S c_{p,S}\frac{\partial T_S}{\partial t}$$

(42)

$$\alpha\rho_{G,0}v_0 c_{p,G}\frac{\partial T_{G,1}}{\partial z} + ha_v\left(T_{G,1} - T_S\right) = 0$$

(43)

$$-\rho_{G,0}v_0 c_{p,G}\frac{\partial T_{G,2}}{\partial z} + ha_v\left(T_{G,2} - T_S\right) = 0$$

(44)

$$\alpha\rho_{G,0}v_0\frac{\partial \omega_{G,1}}{\partial z} + k_D a_v \rho_G\left(\omega_{G,1} - \omega_{S,1}\right) = 0$$

(45)

$$-\rho_{G,0}v_0\frac{\partial \omega_{G,2}}{\partial z} + k_D a_v \rho_G\left(\omega_{G,2} - \omega_{S,2}\right) = 0$$

(46)

$$k_D\left(\omega_{G,1} - \omega_{S,1}\right) = M\frac{r_{S,1}}{\rho_G}$$

(47)

$$k_D\left(\omega_{G,2} - \omega_{S,2}\right) = M\frac{r_{S,2}}{\rho_G}$$

(48)

where $\varphi(z) = 0$ in the inert section ($0 < z < L_{in}$) and $\varphi(z) = 1$ in the catalytic section ($L_{in} \leq z \leq L = L_{in} + L_{cat}$) of the reactor. The boundary conditions for the mass balances are:

$$\begin{cases} \omega_{G,1}\big|_{z=0} = \omega_{G,0} \\ \omega_{G,2}\big|_{z=L} = \alpha\omega_{G,1}\big|_{z=L} \end{cases}$$

(49)

while the boundary conditions for the thermal balances are:

$$\begin{cases} T_{G,1}\big|_{z=0} = T_{G,0} \\ T_{G,2}\big|_{z=L} = \dfrac{\alpha}{\left(1+N'\right)}T_{G,1}\big|_{z=L} + \dfrac{\left(1+N'-\alpha\right)}{\left(1+N'\right)}T_{G,0} + \dfrac{1}{\left(1+N'\right)\rho_{G,0}v_0 c_{p,G}S}Q_{el} \\ \dfrac{\partial T_S}{\partial z}\bigg|_{z=0} = \dfrac{\partial T_S}{\partial z}\bigg|_{z=L} = 0 \end{cases}$$

(50)

where N' is the number of transfer units that accounts for heat loss in the

central chamber.

Appendix 2

If the assumption about the identity of the numbers of Nusselt and Sherwood and the numbers of Schmidt and Prandtl does not hold, the balance equations describing the dynamics of the inert section of the countercurrent reactor (eq. (1)) does not change, as well as their boundary conditions (eq. (3)), while the balance equations for the catalytic section (eq. (4)) are slightly modified: in particular the mass balance equations for the gas phase and for the catalyst surface change:

$$\alpha \frac{\partial \omega_{G,1,cat}}{\partial x_{cat}} + F \cdot Pe_{cat} \omega_{G,1,cat} = 0$$

$$F \cdot Pe_{cat} \omega_{G,1,cat} = \frac{Ma_v L_{cat}}{\rho_{G,0} v_0} r_{S,1}$$

(51)

where $F = \dfrac{h}{k_D c_{p,G} \rho_G}$.

The boundary conditions for the mass balances and for the thermal balances remain the same (eq. (6)).

Appendix 3

$$A(\alpha) = \begin{bmatrix} A_{11} & A_{12} \\ A_{21} & A_{22} \end{bmatrix}$$

$$A_{11}(i,j) = \left[\left(a_{in} B_{i,0,in} + b_{in} A_{i,0,in} \right) p_2 A_{0,j,in} + \left(a_{in} B_{i,j,in} + b_{in} A_{i,j,in} \right) \right] +$$
$$+ \left[\left(a_{in} B_{i,0,in} + b_{in} A_{i,0,in} \right) p_2 A_{0,n_{in}+1,in} + \left(a_{in} B_{i,n_{in}+1,in} + b_{in} A_{i,n_{in}+1,in} \right) \right] \cdot$$
$$\cdot p_6 p_5 \left[\frac{L^* A_{n_{in}+1,0,in}}{\left(A_{0,0,cat} - L^* A_{n_{in}+1,n_{in}+1,in} \right)} p_2 A_{0,j,in} + \frac{L^* A_{n_{in}+1,j,in}}{\left(A_{0,0,cat} - L^* A_{n_{in}+1,n_{in}+1,in} \right)} \right]$$

$$A_{12}(i,j) = \left[\left(a_{in} B_{i,0,in} + b_{in} A_{i,0,in} \right) p_2 A_{0,n_{in}+1,in} + \left(a_{in} B_{i,n_{in}+1,in} + b_{in} A_{i,n_{in}+1,in} \right) \right] \cdot$$
$$\cdot \left[\frac{p_5 L^* A_{0,n_{cat}+1,cat}}{\left(A_{0,0,cat} - L^* A_{n_{in}+1,n_{in}+1,in} \right)} p_3 c_{cat} A_{n_{cat}+1,j,cat} + \frac{p_5 L^* A_{0,j,cat}}{\left(A_{0,0,cat} - L^* A_{n_{in}+1,n_{in}+1,in} \right)} \right]$$

$$A_{21}(i,j) = \left[\left(a_{cat} B_{i,0,cat} + b_{cat} A_{i,0,cat} \right) + \left(a_{cat} B_{i,n_{cat}+1,cat} + b_{cat} A_{i,n_{cat}+1,cat} \right) p_3 c_{cat} A_{n_{cat}+1,0,cat} \right] \cdot$$
$$\cdot p_6 p_5 \left[\frac{L^* A_{n_{in}+1,0,in}}{\left(A_{0,0,cat} - L^* A_{n_{in}+1,n_{in}+1,in} \right)} p_2 A_{0,j,in} + \frac{L^* A_{n_{in}+1,j,in}}{\left(A_{0,0,cat} - L^* A_{n_{in}+1,n_{in}+1,in} \right)} \right]$$

$$A_{22}(i,j) = \left[\left(a_{cat} B_{i,j,cat} + b_{cat} A_{i,j,cat} \right) + \left(a_{cat} B_{i,n_{cat}+1,cat} + b_{cat} A_{i,n_{cat}+1,cat} \right) p_3 c_{cat} A_{n_{cat}+1,j,cat} \right] +$$
$$- \left[\left(a_{cat} B_{i,0,cat} + b_{cat} A_{i,0,cat} \right) + \left(a_{cat} B_{i,n_{cat}+1,cat} + b_{cat} A_{i,n_{cat}+1,cat} \right) p_3 c_{cat} A_{n_{cat}+1,0,cat} \right] \cdot$$
$$\cdot p_6 \left[\frac{p_5 A_{0,n_{cat}+1,cat}}{\left(A_{0,0,cat} - L^* A_{n_{in}+1,n_{in}+1,in} \right)} p_3 c_{cat} A_{n_{cat}+1,j,cat} + \frac{p_5 A_{0,j,cat}}{\left(A_{0,0,cat} - L^* A_{n_{in}+1,n_{in}+1,in} \right)} \right]$$

$$B_1(\alpha) = \begin{bmatrix} B_{11} \\ B_{12} \end{bmatrix}$$

$$B_{11}(i) = \left[\left(a_{in} B_{i,0,in} + b_{in} A_{i,0,in} \right) p_2 A_{0,n_{in}+1,in} + \left(a_{in} B_{i,n_{in}+1,in} + b_{in} A_{i,n_{in}+1,in} \right) \right] p_7 +$$
$$+ \left(a_{in} B_{i,0,in} + b_{in} A_{i,0,in} \right) p_1$$

$$B_{12}(i) = p_7 \left[\left(a_{cat} B_{i,0,cat} + b_{cat} A_{i,0,cat} \right) + \left(a_{cat} B_{i,n_{cat}+1,cat} + b_{cat} A_{i,n_{cat}+1,cat} \right) p_3 c_{cat} A_{n_{cat}+1,0,cat} \right] +$$
$$+ \left(a_{cat} B_{i,n_{cat}+1,cat} + b_{cat} A_{i,n_{cat}+1,cat} \right) p_3$$

$$B_2(\alpha) = \begin{bmatrix} B_{21} \\ B_{22} \end{bmatrix}$$

$$B_{21}(i) = -\left[\left(a_{in}B_{i,0,in} + b_{in}A_{i,0,in}\right)p_2 A_{0,n_{in}+1,in} + \left(a_{in}B_{i,n_{in}+1,in} + b_{in}A_{i,n_{in}+1,in}\right)\right]p_8$$

$$B_{22}(i) = -p_8\left[\left(a_{cat}B_{i,0,cat} + b_{cat}A_{i,0,cat}\right) + \left(a_{cat}B_{i,n_{cat}+1,cat} + b_{cat}A_{i,n_{cat}+1,cat}\right)p_3 c_{cat} A_{n_{cat}+1,0,cat}\right] +$$
$$+ \left(a_{cat}B_{i,n_{cat}+1,cat} + b_{cat}A_{i,n_{cat}+1,cat}\right)p_4$$

$$E(\alpha) = \begin{bmatrix} E_1 \\ E_2 \end{bmatrix}; \; E_1 \text{ is an array of zero elements of length } n_{in};$$

$$E_2(i) = \frac{Pe_{cat}}{2\tau_{cat}} e^{-Pe_{cat}\frac{x_{i,cat}}{\alpha}} \Delta T_{ad}.$$

$$p_1 = \frac{1}{\left(1 - \dfrac{\alpha}{Pe_{in}} A_{0,0,in}\right)}$$

$$p_2 = \frac{\alpha}{Pe_{in}} p_1$$

$$p_3 = \frac{1}{\left(1 - c_{cat} A_{n_{cat}+1,n_{cat}+1,cat}\right)}$$

$$p_4 = \frac{p_3}{(1 + N' - \alpha)\rho_{G,0} v_0 c_{p,G} S}$$

$$p_5 = \frac{1}{\left[1 - \dfrac{L^* A_{n_{in}+1,0,in}}{\left(A_{0,0,cat} - L^* A_{n_{in}+1,n_{in}+1,in}\right)} p_2 A_{0,n_{in}+1,in}\right]}$$

$$p_6 = \frac{1}{\left(1 + \dfrac{p_5 A_{0,n_{cat}+1,cat}}{\left(A_{0,0,cat} - L^* A_{n_{in}+1,n_{in}+1,in}\right)} p_3 c_{cat} A_{n_{cat}+1,0,cat}\right)}$$

$$p_7 = p_6 \left[\frac{p_5 L^* A_{n_{in}+1,0,in}}{\left(A_{0,0,cat} - L^* A_{n_{in}+1,n_{in}+1,in} \right)} p_1 - \frac{p_5 A_{0,n_{cat}+1,cat}}{\left(A_{0,0,cat} - L^* A_{n_{in}+1,n_{in}+1,in} \right)} p_3 \right]$$

$$p_8 = p_6 \frac{p_5 A_{0,n_{cat}+1,cat}}{\left(A_{0,0,cat} - L^* A_{n_{in}+1,n_{in}+1,in} \right)} p_4$$

$$L^* = \frac{L_{cat}}{L_{in}}$$

List of Figures

Figure 7   Time evolution of the axial solid temperature profile when the controller is active and the feeding concentration varies according to Figure 6.

Figure 1

Figure 2

Inert monolith

Catalytic monolith

Dilution $(1-\alpha)Q$

αQ

Q

Heating

Q_{el}
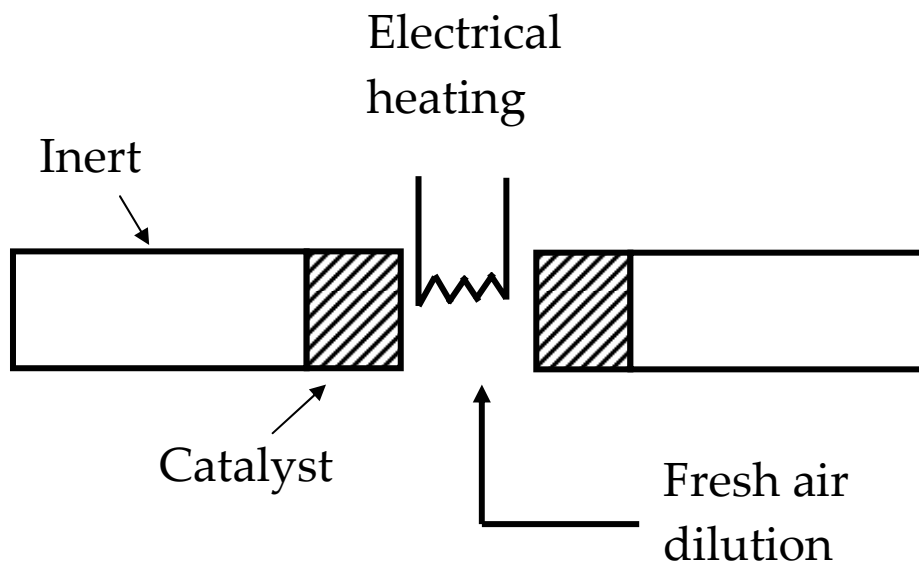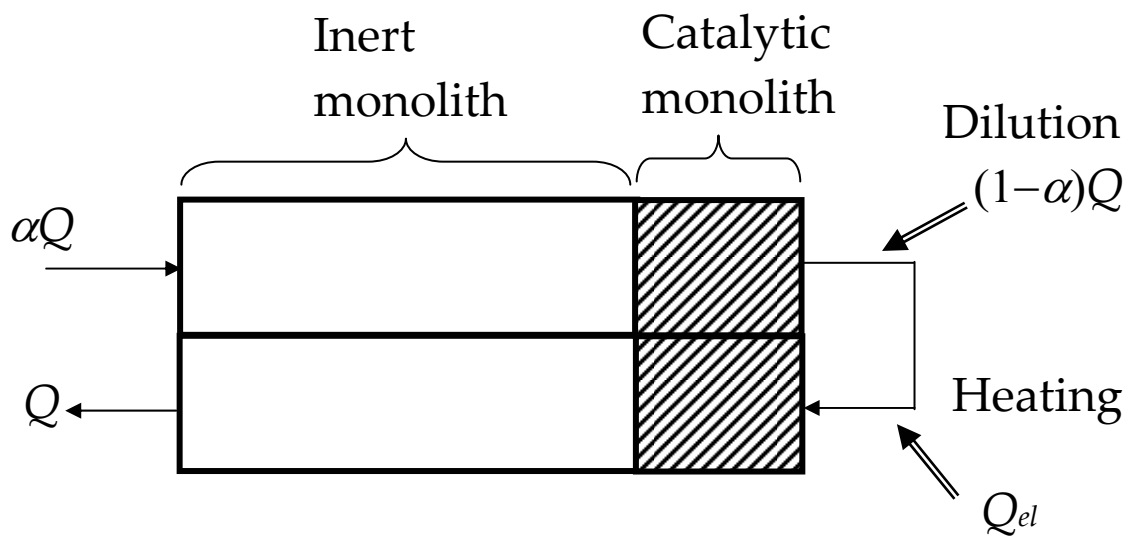
Figure 3

(A)
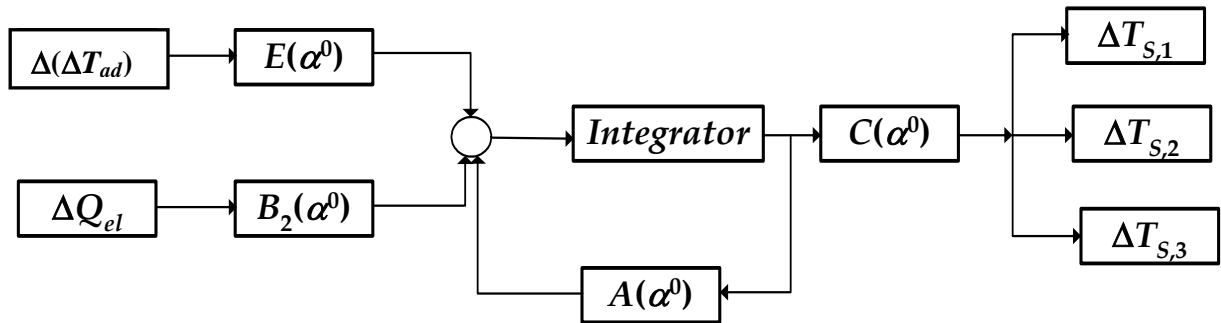
(B)
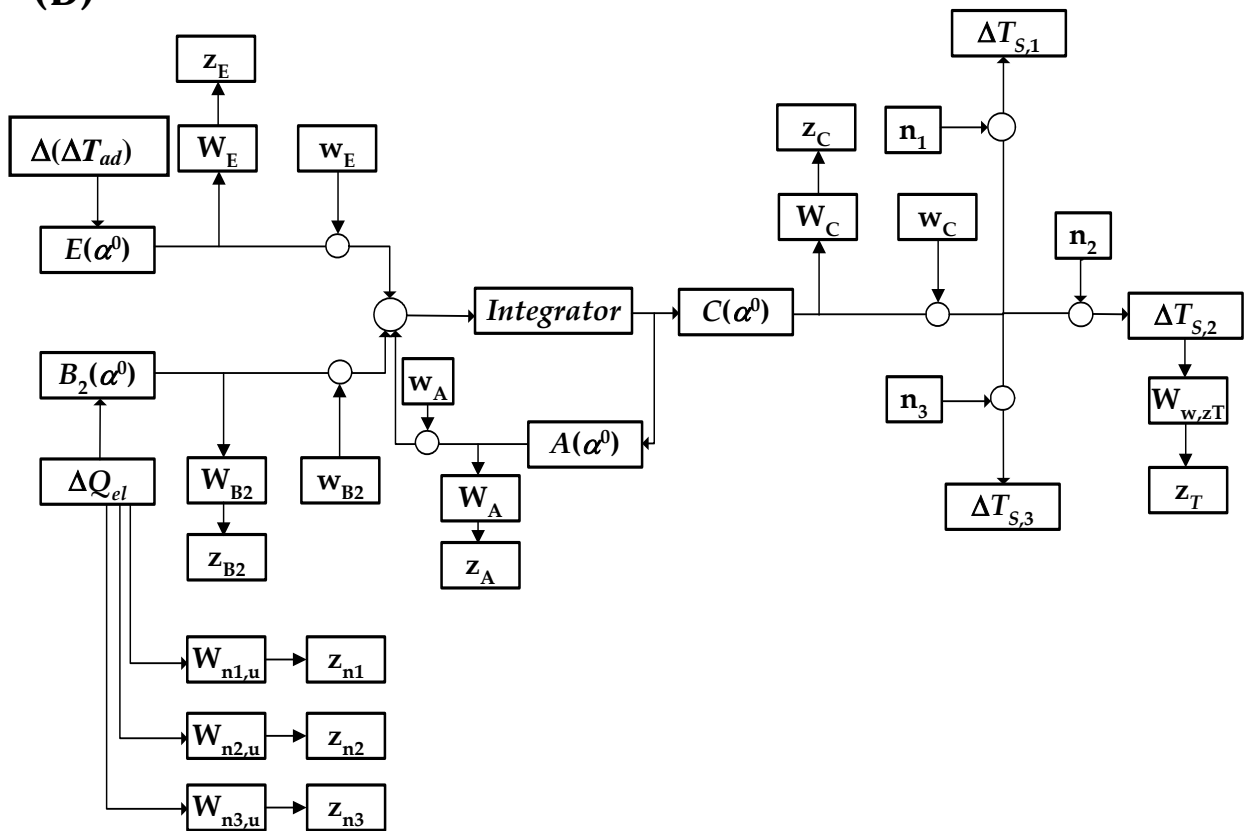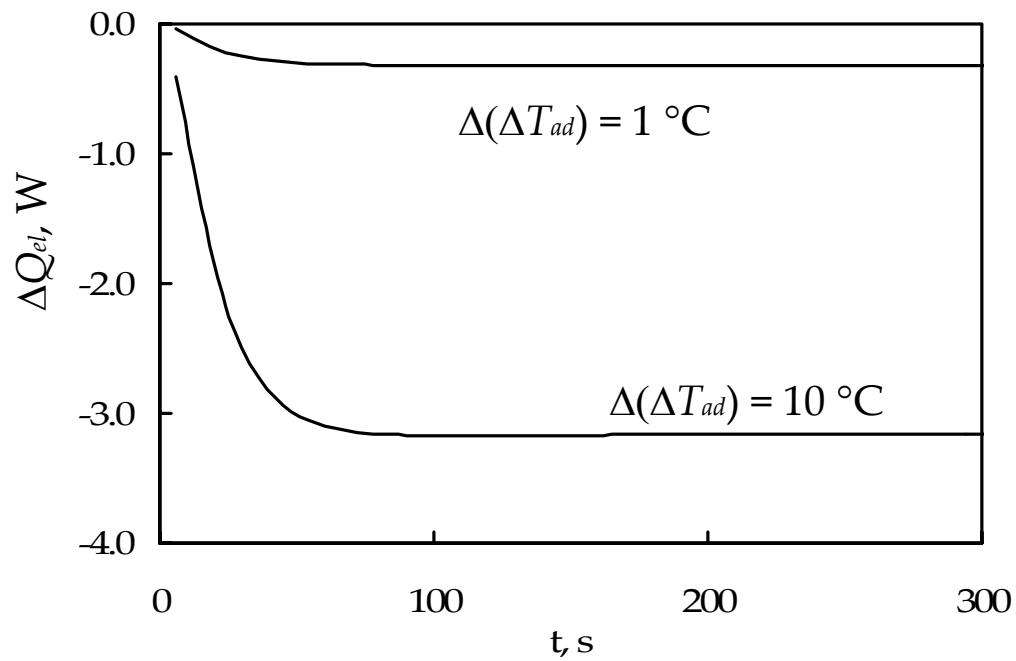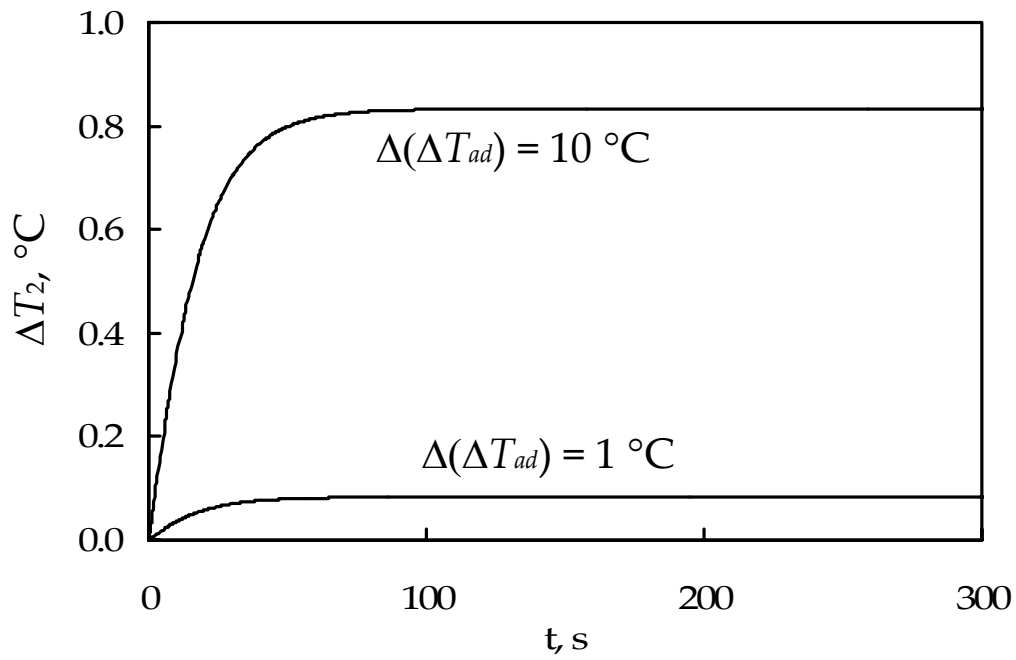
Figure 4

Figure 5

Figure 6

Figure 7